

# Effects of solar UV-B radiation on canopy structure of *Ulva* communities from southern Spain

Kai Bischof<sup>1,5</sup>, Gloria Peralta<sup>2,4</sup>, Gudrun Kräbs<sup>3</sup>, Willem H. van de Poll<sup>1</sup>, José Lucas Pérez-Lloréns<sup>2</sup> and Anneke M. Breeman<sup>1</sup>

<sup>1</sup> University of Groningen, Department of Marine Biology, Kerklaan 30, 9750 AA Haren, The Netherlands

<sup>2</sup> Universidad de Cádiz, Facultad de Ciencias del Mar y Ambientales, 11510 Puerto Real, Spain

<sup>3</sup> Alfred Wegener Institute for Polar and Marine Research, Am Handelshafen 12, D-27570 Bremerhaven, Germany

<sup>4</sup> Netherlands Institute of Ecology, Centre for Estuarine and Coastal Ecology, 4400 AC Yerseke, The Netherlands

Received 26 March 2002; Accepted 11 July 2002

## Abstract

Within the sheltered creeks of Cádiz bay, *Ulva* thalli form extended mat-like canopies. The effect of solar ultraviolet radiation on photosynthetic activity, the composition of photosynthetic and xanthophyll cycle pigments, and the amount of RubisCO, chaperonin 60 (CPN 60), and the induction of DNA damage in *Ulva* aff. *rotundata* Bliding from southern Spain was assessed in the field. Samples collected from the natural community were covered by screening filters, generating different radiation conditions. During daily cycles, individual thalli showed photoinhibitory effects of the natural solar radiation. This inhibition was even more pronounced in samples only exposed to photosynthetically active radiation (PAR). Strongly increased heat dissipation in these samples indicated the activity of regulatory mechanisms involved in dynamic photoinhibition. Adverse effects of UV-B radiation on photosynthesis were only observed in combination with high levels of PAR, indicating the synergistic effects of the two wavelength ranges. In samples exposed either to PAR+UV-A or to UV-B+UV-A without PAR, no inhibition of photosynthetic quantum yield was found in the course of the day. At the natural site, the top layer of the mat-like canopies is generally completely bleached. Artificially designed *Ulva* canopies exhibited fast bleaching of the top layer under the natural solar radiation conditions, while this was not observed in canopies either shielded from UV or from PAR. The bleached first

layer of the canopies acts as a selective UV-B filter, and thus prevents subcanopy thalli from exposure to harmful radiation. This was confirmed by the differences in photosynthetic activity, pigment composition, and the concentration of RubisCO in thalli with different positions within the canopy. In addition, the induction of the stress protein CPN 60 under UV exposure and the low accumulation of DNA damage indicate the presence of physiological protection mechanisms against harmful UV-B. A mechanism of UV-B-induced inhibition of photosynthesis under field conditions is proposed.

Key words: Canopy formation, photosynthesis, ultraviolet radiation, *Ulva rotundata*.

## Introduction

In soft bottom habitats along the shallow coastal zones of southern Spain, *Ulva* thalli are frequently arranged in mat-like canopies (Hernández *et al.*, 1997). The persistence of these structures depends on the degree of water turbulence: in sheltered areas, the canopies may be very stable, keeping their structure during tidal movement as floating thick mats. Within these canopy-like structures, a steep gradient in light climate persists due to self-shading effects (Vergara *et al.*, 1997). The top layer is regularly exposed to high solar radiation, whereas the shaded layers receive reduced light intensities, which are preferably depleted in the blue and the red regions of the spectrum (Vergara *et al.*,

<sup>5</sup> To whom correspondence should be addressed. Fax: +31 50 363 2261. E-mail: K.Bischof@biol.rug.nl

1997). The effect of canopy arrangement on ecophysiology, for example, photoacclimation (Pérez-Lloréns *et al.*, 1996), primary production (Hernández *et al.*, 1997) and photosynthetic performance (Vergara *et al.*, 1997) of *Ulva* species has been studied previously, pointing to the importance of canopy arrangement as a key factor in regulating primary production. However, in these studies, the effect of UV radiation on *Ulva* canopies has been neglected, although harmful UV-B levels are particularly high in southern Spain and, moreover, persisting under long periods of open sky conditions (Altamirano *et al.*, 2000a, b).

The harmful effects of solar UV-B exposure include damage to proteins, pigments and nucleic acids, thus significantly impairing photosynthesis (see Vass, 1997, for a review) and growth. However, the knowledge about how protective mechanisms enable algae from the intertidal and upper sublittoral zones resist high levels of UV-B is still limited. One strategy is adequate shielding against solar exposure, which might be achieved on an intracellular basis (e.g. by internal screening compounds, as described for the mycosporine-like amino acids of red algae; Karsten *et al.*, 1998, 1999) or an extracellular basis, by shading (e.g. within crevices or under canopies). As a particular strategy, the excretion of a UV-absorbing substance was observed in the intertidal green alga *Dasycladus vermicularis* from southern Spain (Gómez *et al.*, 1998; Pérez-Rodríguez *et al.*, 1998). The long-term effects of solar UV radiation on growth and photosynthesis in individual layers of *Ulva rigida* and *U. olivascens* from southern Spain have recently been described by Altamirano *et al.* (2000a, b). In both species, long-term growth was only slightly affected by UV-B radiation, indicating the presence of protective and acclimation mechanisms.

The most obvious indicator of stress (for example, UV-stress) is the loss of pigments, and thus bleaching of the thallus, due to photo-oxidation. Stress related to solar exposure and the steep gradient in light climate within *Ulva* canopies results in an inverse gradient of chlorophyll concentration within the layers forming a mat (Vergara *et al.*, 1998). Further indicators that UV-B stress is beginning have been studied by Cordi *et al.* (1997, 1999) and Bischof *et al.* (2002), revealing that, apart from changes in photosynthetic activity, the activity and concentration of RubisCO, and the activity of the xanthophyll cycle might be altered upon UV exposure.

The aim of the present study was to elucidate the effect of UV-B radiation on the ecophysiology of photosynthesis of *Ulva* canopies and individual thalli under field conditions. Therefore, a wide range of physiological parameters was studied to elucidate the impact of UV from the population down to the protein and DNA level. In addition, the induction of one stress protein (the chaperonin 60, CPN 60), the so-called RubisCO binding protein, was studied as an example of a possible protective mechanism in algae

exposed to UV-B. The changes in the parameters studied were followed over daily cycles, and within artificially designed canopies, giving an insight into how UV-B exposure contributes to the common phenomenon of canopy arrangement in soft bottom habitats along the southern coast of Spain.

## Materials and methods

### Study site

The experiment was conducted between 25 July and 25 August 2001 in the 'Salinas de la Calavera' (36°25' N, 6°13' W; property of Acuinovala, San Fernando, Spain) within the 'Parque Natural Bahía de Cádiz', Spain. The site consists of various parallel creeks, which are interconnected by tidal channels. Tides are semi-diurnal with an average tidal range of 0.8 m. The soil is formed of sedimentary stones with an extended soft bottom layer (up to 0.5 m). Within the chosen central creek, the salinity varied between 34–40 PSU depending on the tidal conditions. The water temperature changed with respect to the tidal conditions and solar insulation and was in the range of 22–27 °C. The vertical attenuation coefficients ( $K_d$ ) of downward photosynthetically active radiation (PAR) varied between 0.6 and 1.0 m<sup>-1</sup>, as determined by parallel irradiance measurements conducted at different water depths, using two cosine-corrected flathead underwater sensors (Li 192 SA, Li-Cor Quantum, Lincoln, USA) connected to a Li-Cor Li-1000 datalogger. During the experimental period, sunny conditions prevailed. Under these conditions, maximal solar irradiance of up to 500 W m<sup>-2</sup> PAR (400–700 nm), 80 W m<sup>-2</sup> UV-A (315–400 nm) and 1.8 W m<sup>-2</sup> UV-B (280–315 nm) were measured (data from continuous UV-measurements from southern Spain can be downloaded from [www.eldonet.org](http://www.eldonet.org)). The continuous monitoring of solar UV-B and temperature was conducted underwater and at ground level using two Eluv-14 dataloggers (developed at the Alfred Wegener Institute, Bremerhaven, Germany; see El Naggar *et al.*, 1995, for reference).

### Algal material

The study site was densely populated by *Ulva* aff. *rotundata* Bliding (identification by JJ Vergara, University of Cádiz, Spain). At the natural growth site, these algae usually form extended floating mats. Individual thalli can grow up to a size of 1.5×0.6 m. For the experiments, healthy, well-pigmented tissue from the subcanopy was chosen. For recording the daily cycles of changes in photosynthetic activity, leaf discs 2.3 cm in diameter were cut from the thalli and distributed among the respective experimental treatments (see below); 500 discs were cut per treatment. For designing artificial canopies, large thalli were selected, and four thallus layers were assembled to form one mat (see below).

### Experimental set-up

For recording daily cycles of photosynthetic activity, the leaf discs were exposed under various cut-off filters (Schott, Mainz, Germany), thus generating different spectral exposure conditions. The filters used were WG 280 (cut-off below 280 nm=PAR+UV-A+UV-B treatment), WG 320 (cut-off below 320 nm=PAR+UV-A treatment), GG 400 (cut-off below 400 nm=PAR treatment), and UG-5 (transmitting below 400 and above 680 nm=UV-A+UV-B treatment). The optical properties of the filters are characterized by the transmission spectra shown in Fig. 1. Filters were fixed to plastic boxes containing the algal discs. Holes in the side walls of the boxes allowed water exchange and wooden pieces attached to the boxes allowed the whole set-up to float at the water surface of the creek. The set-up containing the algae was installed during the evening

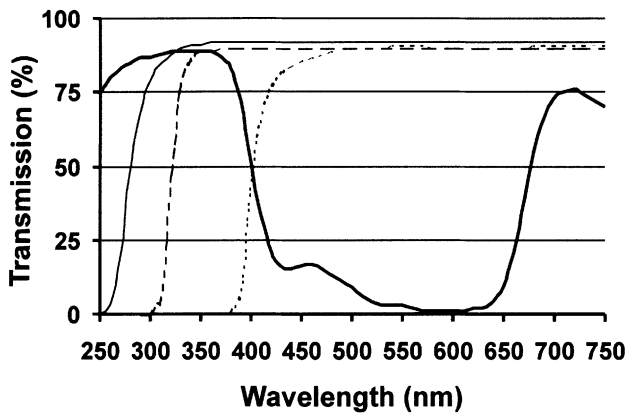


**Fig. 1.** Transmission spectra of the different Schott cut-off filters used: thin solid line: WG 280, dashed line: WG 320, dotted line: GG 400, bold solid line: UG-5 (see Materials and methods for further details).

before the daily cycles were recorded. Sampling was conducted at regular intervals from approximately 07.00 h to 22.00 h. At each sampling, measurements of maximal quantum yield of photosynthesis ( $F_v/F_m$ ) and *PI*-curves were performed, and samples were taken for physiological analyses (pigments and protein content). In the course of the experimental period, the record of daily cycles was repeated three times under comparable radiation conditions, leading to reproducible results. Therefore, as an example, all results shown are for the daily cycle recorded on 2 August 2001.

Artificial *Ulva* canopies were designed as follows: For each mat, four well-pigmented subcanopy layers were arranged between two layers of nylon mesh, cut to the appropriate size to keep the thalli in the desired position. The size of each mat was approximately 22×22 cm. Five different radiation treatments were generated by using filter foils. The filter foils used were: Ultraphan 395 (Digefra, Munich, Germany) to exclude UV-A and UV-B, and Folex 320 (Folex, Dreieich, Germany) to exclude UV-B. Ultraphan 295 was used in order to identify the additional effect of covering samples with the plastic filter foils compared to the samples exposed to unfiltered radiation. The effects of the respective foils on the spectral distribution of solar radiation were previously published by Pérez-Rodríguez *et al.* (1998). Mats were also exposed to unfiltered solar radiation and under UG-5 filters. Six canopies were arranged per treatment and exposed independently. In addition, canopies exposed to unfiltered solar radiation were equipped with biological UV-dosimeters (Viospor, Biosense, Germany; see Quintern *et al.* (1992) and Furusawa *et al.* (1998) for reference) under layers one, two and three. The individual arrangements were attached to a floating system, which guaranteed an even exposure of material at the water surface and the proper positioning of canopies during the time of exposure. After 3 d of exposure, the respective layers of canopies from the different radiation treatments were separated and individually analysed for photosynthetic activity ( $F_v/F_m$  and *PI*-curves) and sampled for physiological analyses (pigments, proteins and DNA damage).

#### Biological variables

The measurements of maximal quantum yield of photosynthesis ( $F_v/F_m$ ) were conducted using a PAM 2000 (Walz, Effeltrich, Germany) chlorophyll fluorometer. Samples were dark acclimated within a black plastic box with a hole in the lid to insert the fiberoptic of the fluorometer. After a 5 s far-red pulse, samples were kept in the

dark for a further 5 min. Ground fluorescence ( $F_o$ ) was determined by the irradiation of samples with a weak pulsed measuring beam ( $0.5 \mu\text{mol m}^{-2} \text{s}^{-1}$  at 650 nm), subsequently, maximal fluorescence ( $F_m$ ) was measured by providing a 0.8 s saturating pulse of white light emitted from a tungsten halogen lamp ( $4000 \mu\text{mol m}^{-2} \text{s}^{-1}$ ). Each determination of  $F_v/F_m$  was conducted using five independent replicates. Relative electron transport rate (*ETR*) versus irradiance curves (*PI*-curves) were recorded according to procedures described by Schreiber *et al.* (1994) and Bischof *et al.* (2000). As the actinic light source, the halogen lamp integrated in the fluorometer was used; actinic irradiance ranged from 65–3000  $\mu\text{mol m}^{-2} \text{s}^{-1}$ . From recorded curves, the parameters  $ETR_{\text{max}}$  (maximal relative electron transport rate),  $q_p$  (photochemical quenching), and  $q_n$  (non-photochemical quenching) were extracted. Due to the time needed to conduct the measurement, only one curve could be recorded under each sampling condition in the course of the day. However, repeated records of daily cycles and the individual analysis of replicate canopies, revealed the representativeness of recorded curves.

Changes in photosynthetic (chlorophyll *a+b*,  $\beta$ -carotene, lutein) and the xanthophyll cycle pigment (violaxanthin [*V*], antheraxanthin [*A*], zeaxanthin [*Z*]) composition were analysed as described by Bischof *et al.* (2002). Pigment data were obtained from independent triplicate samples. From the obtained data, the epoxidation state of the xanthophyll cycle (*EPS*) was calculated as:

$$EPS = (V + 0.5A) / (V + A + Z)$$

(Thayer and Björkman (1990).

In addition, spectra of *in vivo* thallus absorption in the range of 260–750 nm were recorded from three independent replicates by a spectrophotometer (UV2, Unicam, Cambridge, UK).

Crude extracts of samples for protein analysis were prepared, and protein separation by SDS-gel electrophoresis and the subsequent detection of the large subunit of RubisCO by Western blotting was conducted according to Bischof *et al.* (2002). The detection of CPN 60 was performed after Western blotting of SDS-gels using a polyclonal antibody against GroEL from *E. coli*, raised in rabbits. Pilot experiments confirmed the efficient cross-linking of antibodies with CPN 60 from a wide range of marine algae (EG Vrieling, University of Groningen, personal communication). Secondary immunodecoration was performed using an alkaline phosphatase-conjugated goat anti-rabbit antibody. For quantification, blots were scanned with a GS-700 densitometer (Bio-Rad, Hercules, USA) and differences in the abundance of RubisCO and CPN 60 were analysed with image analysis software (Multi-Analyst, Bio-Rad).

Accumulation of DNA damage in artificial canopies, measured as the presence of cyclobutane pyrimidine dimers (CPDs), was measured as described by van de Poll *et al.* (2001).

#### Data treatment

Means and standard deviations were calculated from the respective replicates. Statistical significance of difference was separately tested with respect to the different radiation treatments and to the different positions of thalli within artificial canopies by model I ANOVAs ( $p < 0.05$ ) and Tukey *post-hoc* tests (Sokal and Rohlf, 1995).

## Results

### Daily cycles

Individual thalli exposed to the whole range of solar radiation (WG 280) exhibited a pronounced midday inhibition of maximal quantum yield of photosynthesis ( $F_v/F_m$ ), which was reversed as soon as the solar radiation decreased in the course of the afternoon (Fig. 2). Samples

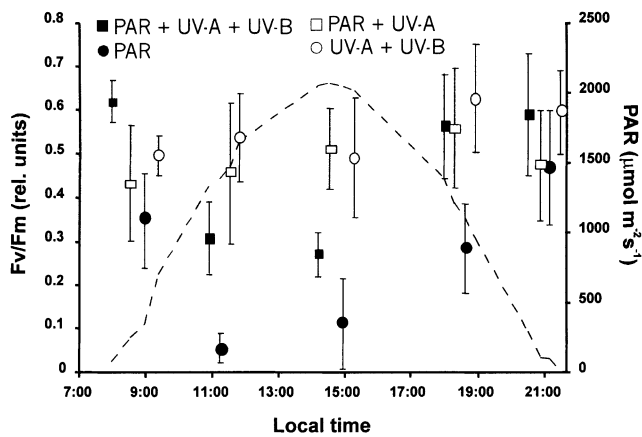


Fig. 2. Daily cycle of maximal quantum yield ( $F_v/F_m$ ) of photosynthesis under different radiation conditions, as recorded on 2 August 2001: (closed squares) PAR+UV-A+UV-B (=WG 280 filter), (open squares) PAR+UV-A (=WG 320 filter), (closed circles) PAR (=GG 400 filter), (open circles) UV-A+UV-B (=UG-5 filter);  $n=5 \pm$ SD. Dashed line marks the course of solar PAR.

kept under UV-exclusion (GG 400 filter) exhibited an even more pronounced inhibition of quantum yield at midday ( $p < 0.05$ ), but with a similar recovering capacity. Interestingly, the algae kept under UV-B exclusion, but receiving UV-A (WG 320 filter), and also the samples shielded from solar PAR, but receiving the whole UV range (UG-5 filter), did not exhibit significant variations in maximal quantum yield in the course of the day.

PI-curves recorded in the early afternoon, the time of most pronounced differences in maximal quantum yield between radiation treatments, indicated differences in the utilization of light energy under the different radiation conditions (Fig. 3). Samples exposed under the WG 320 filter (PAR+UV-A) exhibited the highest  $ETR_{max}$  levels and inhibition of photosynthesis only occurred at irradiances above approximately  $1900 \mu\text{mol m}^{-2} \text{s}^{-1}$  PAR, resulting in a slight increase in non-photochemical quenching ( $q_n$ ). Samples kept under the GG 400 filter (PAR) exhibited a pronounced stimulation of  $q_n$ . Consequently, quantum efficiency and  $ETR_{max}$  were diminished. The samples receiving the whole range of solar radiation (WG 280 filter) showed a somewhat intermediate response. The increase in  $q_n$  was lower and  $ETR_{max}$  levels were higher under high actinic irradiance. In accordance with the differences in  $q_n$ , the course of instantaneous fluorescence ( $F_i$ ) and photochemical quenching ( $q_p$ ) also differed with respect to the previous exposure conditions.

Daily cycles of effects of solar radiation were recorded using healthy, well-pigmented tissue, but the samples became bleached in the course of the experiment. This bleaching proceeded substantially faster in samples exposed to the whole spectrum (WG 280) than under

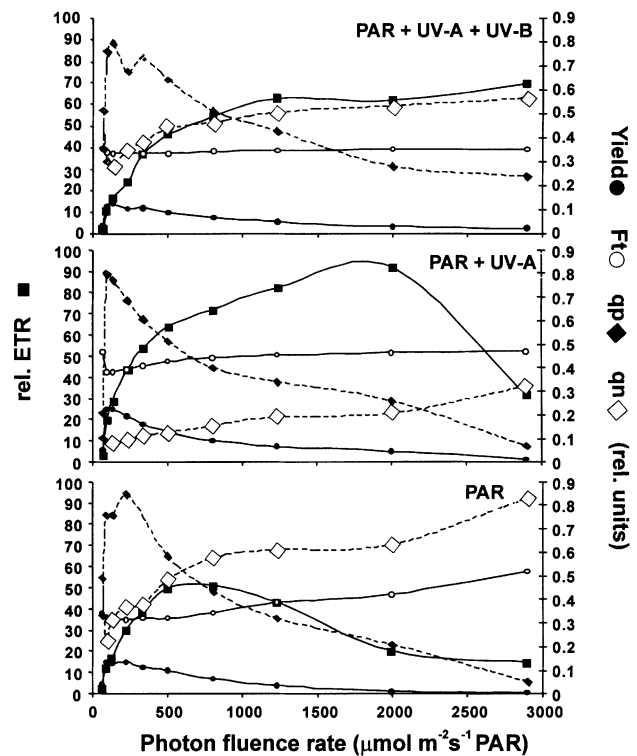


Fig. 3. Examples of PI-curves recorded in samples under WG 280 (=PAR+UV-A+UV-B), WG 320 (=PAR+UV-A), GG 400 (=PAR) filters during the daily cycle recorded on 2 August 2001; samples were collected from 14.30 h to 15.15 h local time. Displayed parameters: (closed squares) relative electron transport rate (rel. ETR), (closed circles) effective quantum yield (yield), (open circles) instantaneous fluorescence ( $F_i$ ), (closed diamonds) photochemical quenching ( $q_p$ ), (open diamonds) non-photochemical quenching ( $q_n$ ).

UV-B exclusion (WG 320). Samples kept either under PAR alone (GG 400) or under UV alone (UG-5) were hardly affected by bleaching (see UV-B induced changes in chlorophyll content in the artificial canopies described below and in Table 1).

#### In vivo thallus absorption

At the study site, *Ulva* populations are commonly arranged in canopies with a markedly bleached top layer and well-pigmented subcanopy specimens. Measurements of *in vivo* thallus absorption were conducted on individual thalli originating from different positions within the natural canopy (Fig. 4). While the well-pigmented subcanopy thalli exhibited the typical absorption spectrum of green algae, the first layer of the natural community only showed marked absorption in the UV-B range, probably originating from the remaining fragments of proteins and nucleic acids. In the wavelength range above 320 nm, absorbance substantially decreased and remained at almost the same level throughout the longer wavelength range. The strong absorbance of UV-B radiation within the respective thallus layers was also confirmed by the results obtained from

**Table 1.** Changes in the content of chlorophyll a, b (Chl a, b),  $\beta$ -carotene and lutein, and in the epoxidation state of violaxanthin (EPS) and the amount of total soluble proteins (TSP), with respect to radiation conditions and position within artificial canopies

Mean values  $\pm$ SD,  $n=3$ . Different letters indicate significant differences among layers within one canopy, asterisks indicate significant differences from initial values.

Sample	Chl a (mg g <sup>-1</sup> FW)	Chl b (mg g <sup>-1</sup> FW)	$\beta$ -carotene (mg mg <sup>-1</sup> Chl a)	Lutein (mg mg <sup>-1</sup> Chl a)	EPS (rel. units)	TSP (mg ml <sup>-1</sup> extract)
Initial						
Subcanopy	0.41 ( $\pm$ 0.11)	0.31 ( $\pm$ 0.09)	0.028 ( $\pm$ 0.005)	0.16 ( $\pm$ 0.03)	0.40 ( $\pm$ 0.06)	1.35 ( $\pm$ 0.41)
Unfiltered						
1st layer	0.04 ( $\pm$ 0.02) a*	0.02 ( $\pm$ 0.02) a*	n.d.	0.14 ( $\pm$ 0.04) a	n.d.	0.23 ( $\pm$ 0.13) a*
2nd layer	0.06 ( $\pm$ 0.04) ab*	0.03 ( $\pm$ 0.02) a*	0.017 ( $\pm$ 0.003) a*	0.22 ( $\pm$ 0.05) a	n.d.	0.21 ( $\pm$ 0.15) a*
3rd layer	0.09 ( $\pm$ 0.04) b*	0.07 ( $\pm$ 0.03) b*	0.016 ( $\pm$ 0.003) a*	0.18 ( $\pm$ 0.05) a	n.d.	0.22 ( $\pm$ 0.18) a*
4th layer	0.18 ( $\pm$ 0.06) c*	0.11 ( $\pm$ 0.03) b*	0.009 ( $\pm$ 0.002) b*	0.19 ( $\pm$ 0.03) a	n.d.	0.32 ( $\pm$ 0.19) a*
295 filter						
1st layer	0.09 ( $\pm$ 0.06) a*	0.05 ( $\pm$ 0.02) a*	0.028 ( $\pm$ 0.007) a	0.16 ( $\pm$ 0.03) a	0.65 ( $\pm$ 0.05) a*	0.37 ( $\pm$ 0.21) a*
2nd layer	0.19 ( $\pm$ 0.05) a*	0.09 ( $\pm$ 0.04) a*	0.031 ( $\pm$ 0.008) a	0.15 ( $\pm$ 0.04) a	0.50 ( $\pm$ 0.06) b	0.48 ( $\pm$ 0.33) ab*
3rd layer	0.48 ( $\pm$ 0.12) b	0.21 ( $\pm$ 0.06) b	0.025 ( $\pm$ 0.006) a	0.17 ( $\pm$ 0.04) a	0.54 ( $\pm$ 0.04) ab	0.61 ( $\pm$ 0.18) ab*
4th layer	0.51 ( $\pm$ 0.11) b	0.29 ( $\pm$ 0.08) b	0.017 ( $\pm$ 0.004) b*	0.16 ( $\pm$ 0.05) a	0.56 ( $\pm$ 0.06) ab	0.89 ( $\pm$ 0.32) b
320 filter						
1st layer	0.23 ( $\pm$ 0.09) a*	0.11 ( $\pm$ 0.03) a*	0.023 ( $\pm$ 0.004) a	0.11 ( $\pm$ 0.02) a	0.50 ( $\pm$ 0.06) a	0.82 ( $\pm$ 0.09) a
2nd layer	0.42 ( $\pm$ 0.10) b	0.20 ( $\pm$ 0.05) b*	0.021 ( $\pm$ 0.005) a	0.13 ( $\pm$ 0.03) a	0.55 ( $\pm$ 0.07) ab	0.98 ( $\pm$ 0.23) ab
3rd layer	0.43 ( $\pm$ 0.12) b	0.22 ( $\pm$ 0.05) b	0.022 ( $\pm$ 0.006) a	0.15 ( $\pm$ 0.03) a	0.64 ( $\pm$ 0.11) b*	1.23 ( $\pm$ 0.11) b
4th layer	0.35 ( $\pm$ 0.09) ab	0.17 ( $\pm$ 0.03) ab*	0.017 ( $\pm$ 0.005) a*	0.17 ( $\pm$ 0.05) a	0.69 ( $\pm$ 0.08) b*	1.18 ( $\pm$ 0.25) b
395 filter						
1st layer	0.26 ( $\pm$ 0.07) a	0.15 ( $\pm$ 0.03) a*	0.018 ( $\pm$ 0.005) a	0.17 ( $\pm$ 0.05) a	0.40 ( $\pm$ 0.03) a	0.83 ( $\pm$ 0.09) a
2nd layer	0.32 ( $\pm$ 0.09) ab	0.16 ( $\pm$ 0.04) a*	0.023 ( $\pm$ 0.006) a	0.16 ( $\pm$ 0.06) a	0.52 ( $\pm$ 0.05) b	0.95 ( $\pm$ 0.19) a
3rd layer	0.38 ( $\pm$ 0.10) ab	0.19 ( $\pm$ 0.06) a	0.021 ( $\pm$ 0.006) a	0.16 ( $\pm$ 0.04) a	0.66 ( $\pm$ 0.11) b*	1.03 ( $\pm$ 0.46) a
4th layer	0.47 ( $\pm$ 0.13) b	0.28 ( $\pm$ 0.07) b	0.016 ( $\pm$ 0.005) a*	0.17 ( $\pm$ 0.06) a	0.62 ( $\pm$ 0.07) b*	1.14 ( $\pm$ 0.39) a
UG-5 filter						
1st layer	0.50 ( $\pm$ 0.11) a	0.27 ( $\pm$ 0.08) a	0.021 ( $\pm$ 0.006) a	0.15 ( $\pm$ 0.07) a	0.73 ( $\pm$ 0.09) a*	1.21 ( $\pm$ 0.41) a
2nd layer	0.53 ( $\pm$ 0.12) a	0.27 ( $\pm$ 0.09) a	0.018 ( $\pm$ 0.003) a	0.15 ( $\pm$ 0.06) a	0.71 ( $\pm$ 0.10) a*	1.18 ( $\pm$ 0.17) a
3rd layer	0.67 ( $\pm$ 0.14) a*	0.35 ( $\pm$ 0.11) a	0.017 ( $\pm$ 0.004) a	0.14 ( $\pm$ 0.05) a	0.64 ( $\pm$ 0.08) a*	1.19 ( $\pm$ 0.22) a
4th layer	0.69 ( $\pm$ 0.14) a*	0.34 ( $\pm$ 0.12) a	0.021 ( $\pm$ 0.007) a	0.13 ( $\pm$ 0.06) a	0.69 ( $\pm$ 0.09) a*	1.11 ( $\pm$ 0.38) a

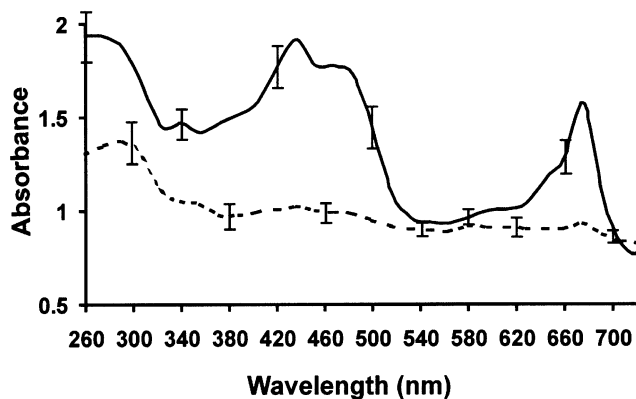


**Fig. 4.** *In vivo* thallus absorption of well-pigmented subcanopy layers of *U. rotundata* (solid line) and bleached top layers taken from the natural community (dashed line);  $n=3 \pm$ SD displayed at 80 nm steps.

biological dosimeters (Viospor) installed within artificially designed mats, compared to continuous UV-measurements in the atmosphere (Eluv-14). Results from both types of dosimeters were weighted to the MED (minimal erythemal dose) function and reveal that after 3 d of exposure, only 3.7% of the atmospheric fluence of this particularly harmful radiation in the UV-B range was transmitted through the first thallus layer.

#### Artificial canopies

Photosynthetic activity and pigment composition were differentially affected with respect to the position of thalli. Mats exposed under the UG-5 filter (UV-A+UV-B) and the 320 filter (PAR+UV-A) did not show significant inhibition of maximal quantum yield of photosynthesis ( $F_v/F_m$ ), whereas in the top layers exposed to PAR alone (395 filter) maximal quantum yield was inhibited to an intermediate extent (Fig. 5). Mats exposed to the whole spectrum (295 filter and unfiltered) of solar radiation exhibited a steep gradient in  $F_v/F_m$  values, with strongly reduced values in the first layer. This inhibitory effect was even more obvious for the observed *ETR*s (Fig. 6). In the material exposed to PAR+UV-A+UV-B, high photosynthetic activities could only be observed in the third and fourth layers from top. Results obtained from the other radiation treatments did not show these drastic differences between the top and subcanopy layers (data not shown).

After 3 d of exposure, changes in the concentration of chlorophyll (Chl) *a* and *b* with the position of the layers in the canopy could be observed under most radiation treatments (Table 1). Compared to the initial values, the most drastic loss of Chl *a* and *b* could be observed in the mats exposed to unfiltered solar radiation ( $P < 0.05$ ), whereas in the samples under the 295 filter a steep gradient

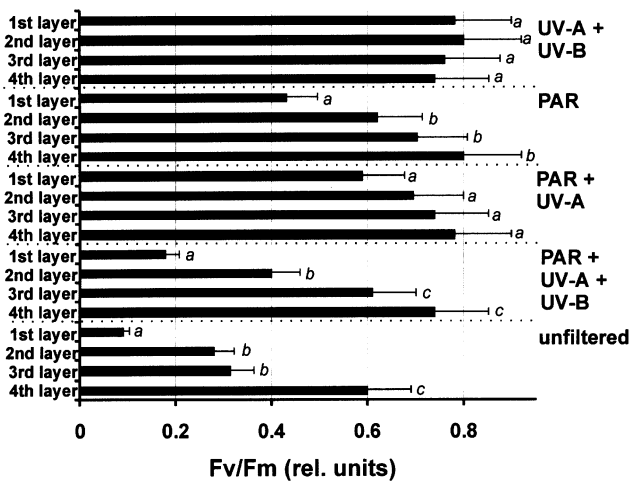


Fig. 5. Maximal quantum yield of photosynthesis ( $F_v/F_m$ ) of thalli forming different layers within artificially generated *Ulva* canopies, with respect to radiation conditions and position in the canopy, after 3 d of exposure;  $n=5 \pm$ SD. Radiation treatments: UV-A+UV-B (=UG-5 filter), PAR (=Ultraplan 395), PAR+UV-A (=Folex 320), PAR+UV-A+UV-B (=Ultraplan 295), and unfiltered solar radiation. Different letters indicate significant differences among layers within one canopy.

in Chl concentration was found. In the mats exposed under the 320 and 395 filters, only a minor loss of Chl was observed in the first layer. Under the UG-5 filter all thallus layers exhibited elevated Chl concentrations compared to the initial samples. Marked differences in lutein and  $\beta$ -carotene content were neither found with respect to radiation conditions nor with respect to the position of thalli within the canopies, when concentrations were calculated based on chlorophyll content (Table 1).

The analysis of the xanthophyll cycle pigments exhibited significant differences in the epoxidation state (EPS) of violaxanthin in the first layer of the mats under the 395 and 295 filter (Table 1): the EPS found in the thalli forming the first layer under the 295 filter was significantly higher than under the 395 filter ( $p < 0.05$ ). In the first thallus layer under the 320 filter, an intermediate EPS value was measured, whereas under the UG-5 filter the highest EPS was found.

Within artificially designed canopies, strong losses of soluble proteins were observed under UV-B exposure (unfiltered and 295 filter). This effect was less pronounced in the samples either kept under the 320 or 395 filter (Table 1). Samples under the UG-5 filter did not show adverse effects of UV-B on protein content, when compared to the initial samples.

A significant loss of RubisCO was observed within the first two layers under exposure to PAR+UV-A+UV-B ( $p < 0.05$ ; Fig. 7, left). Under the 320 and 395 filters, RubisCO concentrations were only slightly reduced compared to the initial values. Again, samples excluding PAR and only receiving UV did not show reduced RubisCO concentra-

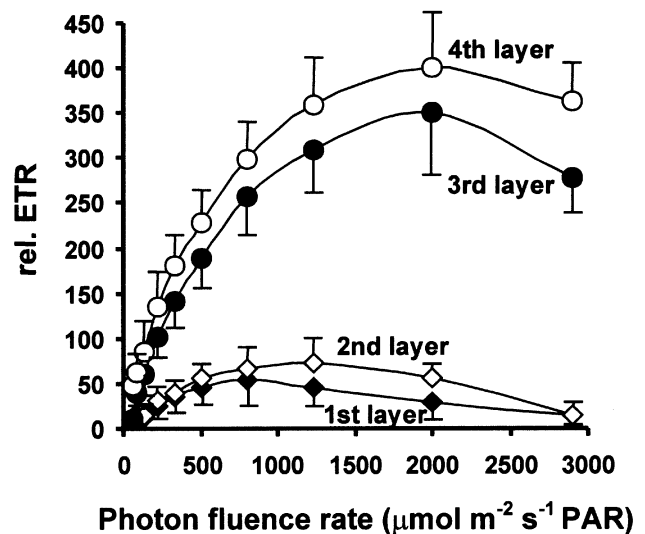


Fig. 6. PI-curves showing relative electron transport rates (rel. ETR) of different thallus layers of artificially generated *Ulva* canopies after being exposed to unfiltered solar radiation for 3 d. Results were pooled from PI-curves recorded in four independently exposed canopy arrangements,  $\pm$ SD.

tions. Comparing the changes in RubisCO concentrations to the variations of  $\arcsin$ -transformed  $F_v/F_m$  values revealed a linear relationship between these two parameters ( $y=7.8x+1.0598$ ;  $r^2=0.871$ ).

Within the artificial canopies, there were elevated concentrations of CPN 60 in the first layers of almost all the treatments (Fig. 7, right), but not in the samples exposed to the unfiltered radiation, in which the top layers were regarded as being physiologically dead. The concentration of CPN 60 was highest in the first layer of mats kept under the 395 and UG-5 filters, with the most pronounced induction observed under the latter treatment.

Finally, the accumulation of DNA damage (CPDs) was measured in canopies exposed under unfiltered solar radiation (Fig. 8). Thalli forming mats exposed to the unfiltered solar radiation exhibited low CPD concentrations, with a gradient of CPDs with respect to their position within the canopy. Values ranged from 1.88 ( $\pm 0.223$ ) CPDs per one million bases in the top layer to 1.0 ( $\pm 0.366$ ) CPDs in the fourth layer. In the initially collected samples from the subcanopy 0.65 ( $\pm 0.354$ ) CPDs were measured.

## Discussion

These results reveal a strong contribution of solar UV-B to the inhibition of *in situ*-photosynthesis and to the typical structure of canopy arrangement. However, in this study's experiments, UV-B only exerted adverse effects in combination with high levels of PAR.

In both experimental set-ups, the daily cycles and artificial mats, photosynthetic quantum efficiencies were not adversely affected under the UG-5 filter, whereas an

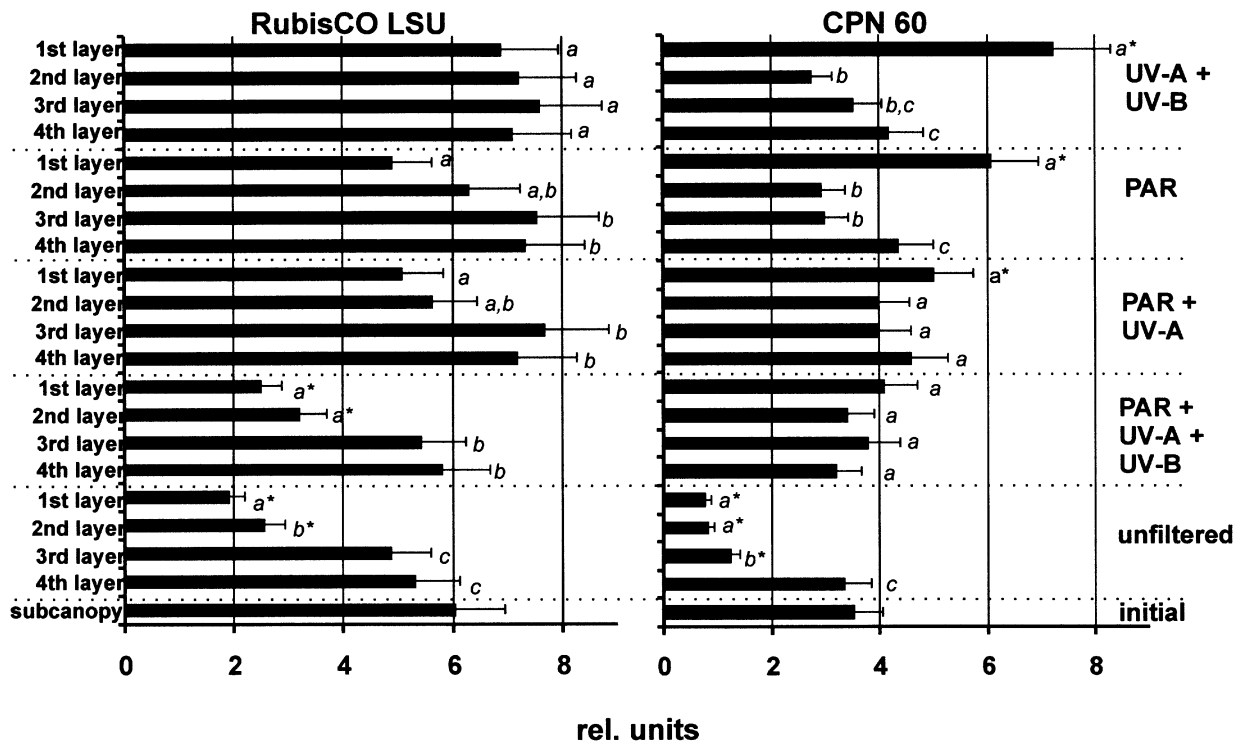


**Fig. 7.** (Left) changes in the abundance of the large subunit of RubisCO; (Right) changes in the concentration of CPN 60 with respect to radiation conditions and position in the canopy, as determined by western blotting and densitometry;  $n=4 \pm SD$ . Radiation treatments: UV-A+UV-B (=UG-5 filter), PAR (=Ultraplan 395), PAR+UV-A (=Folex 320), PAR+UV-A+UV-B (=Ultraplan 295), unfiltered solar radiation, and initially sampled material taken from the subcanopy. Different letters indicate significant differences among layers within one canopy, asterisks indicate significant differences from initial values.

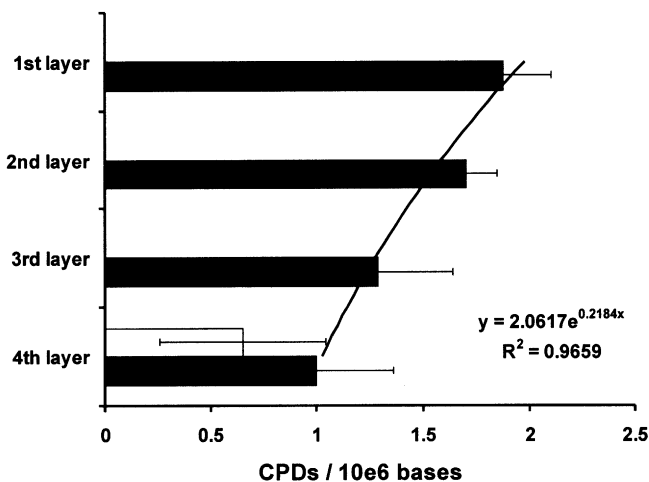


**Fig. 8.** Accumulation of cyclobutane pyrimidine dimers (CPDs) in the DNA, with respect to position in the canopy exposed to unfiltered solar radiation, white bar represents CPD levels in the initially sampled subcanopy layers;  $n=3 \pm SD$ .

inhibition of photosynthesis was observed in samples receiving either PAR+UV or PAR alone (Figs 2, 5), a response previously observed in intertidal brown algae from the Arctic (Bischof *et al.*, 2001). Persistent high

quantum yields in samples exposed under the WG 320 filter (Figs 2, 3, 5) may indicate the presence of beneficial effects of the UV-A and blue light regions. It is known from brown algal species that blue light and UV-A may stimulate photosynthesis via the activation of Calvin cycle enzymes (Schmid and Dring, 1996). Provided that comparable mechanisms also occur in green algal species, it is assumed that an enhanced activity of secondary photosynthetic reactions prevented the inhibition of photosynthesis. Beneficial effects of solar UV-A were also found in a field study on the green alga *Dasycladus vermicularis* from southern Spain, in which samples exposed to the solar PAR+UV-A showed less pronounced inhibition and faster recovery of photosynthesis, than samples exposed either to PAR alone or to PAR+UV-A+UV-B, which were both inhibited to a similar degree (Gómez *et al.*, 1998).

In this study, the strong response of algae exposed under UV exclusion compared with samples exposed to the full solar spectrum represents a particular reaction (Fig. 2), which is different from the results obtained for polar and cold-temperate species, in which the UV-B region always led to a stronger inhibition during the daily cycles (Hanelt *et al.*, 1997; Bischof *et al.*, 2001). An explanation for this response might be provided by comparing *PI*-curves and analysing quenching parameters (Fig. 3). The high  $ETR_{max}$

levels in samples exposed under the WG 320 filter (PAR+UV-A) indicate the additional stimulation of photosynthesis by UV-A. In samples kept under the GG 400 filter (PAR only), a strong stimulation of  $q_n$  (Fig. 3) indicates increased heat dissipation of excessively absorbed energy (Havaux *et al.*, 1991; Ruban and Horton, 1994; Young and Frank, 1996). The consequent reduction in quantum efficiency has been described as an important diagnostic characteristic of dynamic photoinhibition (Osmond, 1994). In parallel with the increase in  $q_n$ ,  $ETR$  is strongly diminished, pointing to regulatory mechanisms in response to high solar PAR. In samples receiving the whole range of PAR+UV-A+UV-B, heat dissipation appears not as pronounced, resulting in higher  $ETR_{max}$  levels under high actinic irradiance, indicating an impaired regulatory and defence system against high radiation.

Heat dissipation is related to the activity of the xanthophyll cycle (Frank *et al.*, 1994), which has previously been reported to be impaired under UV-B exposure (Pfündel *et al.*, 1992; Bischof *et al.*, 2002). Within this cycle, excessively absorbed energy is dissipated as heat and thus it prevents electron transfer to oxygen and the subsequent generation of harmful reactive oxygen species during photosynthesis (see Demmig-Adams, 1990, for review). The contribution of the xanthophyll cycle to photoinhibition of photosynthesis and its recovery in *U. rotundata* has been described in detail by Franklin *et al.* (1992). In samples collected during the daily cycles, no statistically significant differences in xanthophyll composition could be observed in this experiment (data not shown). However, the differences in EPS of the top layers under PAR+UV-A+UV-B (295 filter) and PAR alone (395 filter) in the mat experiment indicated a higher share of zeaxanthin and, thus, an activated xanthophyll cycle (Franklin *et al.*, 1992) under UV exclusion (Table 1). The higher EPS found in the first layer under the 295 filter indicates that the conversion of violaxanthin to zeaxanthin is inhibited. These results may also be applied to the data obtained from daily cycles, in which samples exposed under UV exclusion exhibited strongly elevated non-photochemical quenching, indicating the activity of the xanthophyll cycle (Demmig-Adams, 1990). Previously, Bischof *et al.* (2002) described the UV-induced inhibition of the xanthophyll cycle in a field experiment on *Ulva lactuca* from Heligoland (German Bight). UV-B radiation seems to impair this important protective mechanism against high light stress, probably via an inhibition of the enzyme violaxanthin de-epoxidase (Pfündel *et al.*, 1992). Reduced activity of the xanthophyll cycle results in the elevated production of reactive oxygen species (ROS) and, finally, in photo-oxidation of pigments, which is described as a common response of plants towards UV-B exposure (see Vass, 1997, for review). By contrast to samples only exposed to PAR, ROS production may be elevated during exposure to the whole solar spectrum, contributing to

photo-oxidation and bleaching of pigments, as observed in the mat experiment (see Table 1 for changes in pigment composition). The fast bleaching of samples kept under the full range of solar radiation shows that UV-B, beside other factors like temperature, desiccation, and osmotic stress, can be regarded as an important factor in the bleaching and disintegration of the first thallus layers of *Ulva* mats. Indeed, it should be noted here that differences found between the samples exposed to unfiltered radiation compared to those exposed under the 295 filter (Table 1; Figs 5, 7), might partly be attributed to desiccation and osmotic stress, as, in contrast to the treatment without any filter, a thin water layer is always retained between the underside of the foil and the first thallus layer. The data presented here also reveal the strong synergistic effects of UV and PAR affecting Chl concentration, as under the UG-5 filter no reduction in Chl was found at all.

Proteins absorb strongly in the UV-B range, and a loss of proteins has previously been described for macroalgae under UV exposure (see Vass, 1997, for review). Within photosynthesis, RubisCO has been identified as a primary target (Jordan *et al.*, 1992; Bischof *et al.*, 2000). Indeed, these results show a significant loss of RubisCO within the first two layers under exposure to PAR+UV-A+UV-B (Fig. 7, left), but also that samples subjected to no PAR, thus only receiving UV, did not exhibit any reduction in RubisCO concentration. This confirms that, in field-grown plants, only the combination of UV-B and high PAR may harm photosynthesis. Loss of RubisCO concentration may be the result of either UV-B induced destruction of the protein or reduced synthesis due to down-regulation of gene expression (Jordan *et al.*, 1992; A-H-Mackerness *et al.*, 1999; Bischof *et al.*, 2000). Curiously, the presence of ROS has recently been identified as an important component in the signal transduction pathway to down-regulate the expression of *rbcL* upon UV-B exposure (A-H-Mackerness *et al.*, 1999). This may partly explain the unaffected RubisCO concentrations under the UG-5 filter, as photosynthetic activity, which is inevitably linked to ROS generation, is low there, because it is only driven by the low irradiance of incoming red light transmitted by this filter. The relationship between changes in RubisCO concentrations and the variations of *arcsin*-transformed  $F_v/F_m$  values might indicate a closer correlation, although previous studies have shown that UV exposure might impair RubisCO content and activity *prior* to primary photosynthetic reactions (Allen *et al.*, 1997).

In the context of changes in the concentration of RubisCO, the induction of CPN 60 was studied. This plastidic chaperone has been described as the RubisCO-binding protein (Gatenby and Ellis, 1990), facilitating the assembly of the respective subunits of RubisCO. Acting as a stress protein, it may also protect RubisCO from stress-induced degradation, maintaining it in a stable functional state (Schmitz *et al.*, 1996). Chaperonin 60 has previously



been observed to be induced under different kinds of abiotic stress (Jagtap *et al.*, 1998), which include UV exposure (EG Vrieling *et al.*, unpublished data). Increasing concentration of CPN 60 (Fig. 7, right) may also be attributed to the large increase in the irradiance of PAR and also to the temperature at the water surface. However, the induction of CPN 60 was most pronounced in the first layer of mats kept under the UG-5 filter, which points to a strong contribution of UV to its expression. Further studies have to elucidate to what extent the induction of CPN 60 may contribute to the protection of RubisCO under UV-B exposure in the field.

Finally, the accumulation of DNA damage (CPDs) was found to be extremely low (Fig. 8). The absence of pronounced DNA damage in these algae originating from a region with high solar irradiance suggests the presence of efficient protective and/or repair mechanisms and indicates that the previously demonstrated adverse effects were not mediated by this type of damage.

## Conclusions

These results clearly show that adverse UV-B effects on photosynthesis under field conditions mainly occur in combination with high levels of PAR. This can be observed for a variety of physiological reactions, including photosynthetic activity, changes in pigment and protein concentration, and abundance of RubisCO. Taking into account the results of present and previous studies, the following mechanism contributing to the UV-induced inhibition of photosynthesis under field conditions is proposed: amongst others, UV-B may harm protective and regulatory mechanisms such as, for example, the enzymatic violaxanthin de-epoxidation within the xanthophyll cycle as previously shown for isolated chloroplasts and intact leaves (Pfündel *et al.*, 1992), but also for cold temperate macroalgae under field conditions (Bischof *et al.*, 2002). Consequently, algae might not be as capable of responding to the impinging high PAR by an increase in heat dissipation (Demmig-Adams, 1990; Niyogi *et al.*, 1997), which may result in an increased ROS production (Asada and Takahashi, 1987). This may either lead to photo-oxidation of pigments and proteins (Andersson *et al.*, 1992) or down-regulation of gene expression (A-H-Mackerness *et al.*, 1999). The data suggest an important role for ROS in observed effects, rather than DNA damage. Further field studies should focus on the proof of this hypothesis. Photosynthetic data also revealed the contribution of UV-A to maintain high quantum yields in the course of the day. The study of the synergistic effects of the different wavelength ranges (PAR, UV-A, UV-B) and their respective ratios will be an important aspect in future investigations of acclimation mechanisms under a changing light climate.

It is evident that other abiotic factors also contribute to the bleaching of pigments, but from the study presented here it can be concluded that UV-B is one of the driving forces, leading to the bleaching and disintegration of top layers of natural *Ulva* canopies. The selective absorption characteristics of the bleached material (Fig. 4) are responsible for the efficient shielding of the subcanopy algae from UV-B exposure. Therefore, the typical canopy arrangement can also be regarded as an ecological mechanism to avoid healthy and productive material being exposed to UV-B. Hernández *et al.* (1997) proposed canopy formation as a strategy to maintain high production rates. Under field conditions, growth rates up to 30% d<sup>-1</sup> were determined (Hernández *et al.*, 1997) in *Ulva* species from southern Spain, which can, thus, be regarded as following a typical r-strategy. Since these species exhibit very low compensation points for growth (5 μmol m<sup>-2</sup> s<sup>-1</sup>; Pérez-Lloréns *et al.*, 1996) canopies with up to 17 layers can be found in non-wave-exposed areas (Hernández *et al.*, 1997; Vergara *et al.*, 1998). Therefore, bleaching of top layers hardly represents a constraint to primary production on the population level. This study's data indicate that UV-B-induced bleaching of the first layer and shielding of the subcanopy against harmful UV-B is a key factor enabling the mass development of *Ulva* communities, which are frequently observed in eutrophic systems along the southern coast of Spain.

## Acknowledgements

The authors are most grateful to Acuinova for providing access to the saltmarsh system, to Petronila González Vela for the perfect logistic support, and to JJ Vergara and FG Brun for helpful advice and support. Antibodies against RubisCO and CPN 60 were kindly provided by Professor R Scheibe (University of Osnabrück, Germany) and Dr EG Vrieling (University of Groningen, The Netherlands), respectively. Funding of KB by an Emmy Noether fellowship provided by the Deutsche Forschungsgemeinschaft (DFG; project BI 772/1-1) is gratefully acknowledged. Additional support was provided by the Ministerio Espanol de Educacion y Cultura (project MAR 99-0561).

## References

- A-H-Mackerness S, Jordan BR, Thomas B. 1999. Reactive oxygen species in the regulation of photosynthetic genes by ultraviolet radiation (UV-B: 280–320 nm) in green and etiolated buds of pea (*Pisum sativum* L.). *Journal of Photochemistry and Photobiology B: Biology* **48**, 180–188.
- Allen DJ, McKee IF, Farage PK, Baker NR. 1997. Analysis of limitations to CO<sub>2</sub> assimilation on exposure of leaves of two *Brassica napus* cultivars to UV-B. *Plant, Cell and Environment* **20**, 633–640.
- Altamirano M, Flores-Moya A, Figueroa FL. 2000a. Long-term effects of natural sunlight under various ultraviolet radiation conditions on growth and photosynthesis of intertidal *Ulva rigida* (Chlorophyceae) cultivated *in situ*. *Botanica Marina* **43**, 19–26.
- Altamirano M, Flores-Moya A, Figueroa FL. 2000b. Growth seasonality, photosynthetic pigments, and C and N content in

- relation to environmental factors: a field study on *Ulva olivascens* (Ulvales, Chlorophyta). *Phycologia* **39**, 50–58.
- Andersson B, Salter AH, Virgin I, Vass I, Styring S.** 1992. Photodamage to photosystem II—primary and secondary events. *Journal of Photochemistry and Photobiology B: Biology* **15**, 15–31.
- Asada K, Takahashi M.** 1987. Production and scavenging of active oxygen in photosynthesis. In: Kyle DJ, Osmond CB, Arntzen CJ, eds. *Photoinhibition. Topics in photosynthesis*, Vol. 9. Amsterdam: Elsevier Science Publishers, 89–109.
- Bischof K, Hanelt D, Wiencke C.** 2000. Effects of ultraviolet radiation on photosynthesis and related enzyme reactions of marine macroalgae. *Planta* **211**, 555–562.
- Bischof K, Hanelt D, Wiencke C.** 2001. UV-radiation and arctic marine macroalgae. In: Hessen D, ed. *UV-radiation and arctic ecosystems*. Ecological Studies Series, Vol. 153. New York, Berlin, Heidelberg: Springer, 227–243.
- Bischof K, Kräbs G, Wiencke C, Hanelt D.** 2002. Solar ultraviolet radiation affects Rubisco activity and composition of photosynthetic and xanthophyll cycle pigments in the intertidal green alga *Ulva lactuca* L. *Planta* **215**, 502–509.
- Cordi B, Depledge MH, Price DN, Salter LF, Donkin ME.** 1997. Evaluation of chlorophyll fluorescence, *in vivo* spectrophotometric pigment absorption and ion leakage as biomarkers of UV-B exposure in marine macroalgae. *Marine Biology* **130**, 41–49.
- Cordi B, Hyde P, Donkin ME, Price DN, Depledge MH.** 1999. Evaluation of *in vivo* thallus absorbance and chlorophyll fluorescence as biomarkers of UV-B exposure and effects in marine macroalgae from different tidal levels. *Marine Environmental Research* **48**, 193–212.
- Demmig-Adams B.** 1990. Carotenoids and photoprotection in plants: a role for the xanthophyll zeaxanthin. *Biochimica et Biophysica Acta* **1020**, 1–24.
- El Naggat S, Gustat H, Magister H, Rochlitz R.** 1995. An electronic personal UV-B-dosimeter. *Journal of Photochemistry and Photobiology B: Biology* **31**, 83–86.
- Frank HA, Cua A, Chynwat V, Young A, Gosztola D, Wasielewski MR.** 1994. Photophysics of the carotenoids associated with the xanthophyll cycle in photosynthesis. *Photosynthesis Research* **41**, 389–395.
- Franklin LA, Levavasseur G, Osmond CB, Henley WJ, Ramus J.** 1992. Two components of onset and recovery during photoinhibition of *Ulva rotundata*. *Planta* **186**, 399–408.
- Furusawa Y, Quintern LE, Holtzschmidt H, Koepke P, Saito M.** 1998. Determination of the erythema-effective solar radiation in Japan and Germany with a spore monolayer film optimised for the detection of UVB and UVA-results of a field campaign. *Applied Microbiology and Biotechnology* **50**, 597–603.
- Gatenby AA, Ellis RJ.** 1990. Chaperone function: the assembly of ribulose biphosphate carboxylase-oxygenase. *Annual Reviews of Cell Biology* **6**, 125–149.
- Gómez I, Pérez-Rodríguez E, Vinegla B, Figueroa FL, Karsten U.** 1998. Effects of solar radiation on photosynthesis, UV-absorbing compounds and enzyme activities of the green alga *Dasycladus vermicularis* from southern Spain. *Journal of Photochemistry and Photobiology B: Biology* **47**, 46–57.
- Hanelt D, Wiencke C, Nultsch W.** 1997. Influence of UV radiation on the photosynthesis of Arctic macroalgae in the field. *Journal of Photochemistry and Photobiology B: Biology* **38**, 40–47.
- Havaux M, Strasser RJ, Greppin H.** 1991. A theoretical and experimental analysis of the  $q_p$  and  $q_n$  coefficients of chlorophyll fluorescence quenching and their relation to photochemical and non-photochemical events. *Photosynthesis Research* **27**, 41–55.
- Hernández I, Peralta G, Pérez-Lloréns JL, Vergara JJ, Niell FX.** 1997. Biomass and dynamics of growth of *Ulva* species in Palmones river estuary. *Journal of Phycology* **33**, 764–772.
- Jagtap V, Bhargava S, Streb P, Feierabend J.** 1998. Comparative effect of water, heat and light stresses on photosynthetic reactions in *Sorghum bicolor* (L.) Moench. *Journal of Experimental Botany* **49**, 1715–1721.
- Jordan BB, He J, Chow WS, Anderson JM.** 1992. Changes in mRNA levels and polypeptide subunits of ribulose-1,5-bisphosphate carboxylase in response to supplementary ultraviolet-B radiation. *Plant, Cell and Environment* **15**, 91–98.
- Karsten U, Sawall T, Hanelt D, Bischof K, Figueroa FL, Flores-Moya A, Wiencke C.** 1998. An inventory of UV-absorbing mycosporine-like amino acids in macroalgae from polar to warm-temperate regions. *Botanica Marina* **41**, 443–453.
- Karsten U, Bischof K, Hanelt D, Tüg H, Wiencke C.** 1999. The effect of UV-radiation on photosynthesis and UV-absorbing substances in the endemic Arctic macroalga *Devaleraea ramentacea* (Rhodophyta). *Physiologia Plantarum* **105**, 58–66.
- Niyogi KK, Björkman O, Grossman AR.** 1997. The roles of specific xanthophylls in photoprotection. *Proceedings of the National Academy of Sciences, USA* **94**, 14162–14167.
- Osmond CB.** 1994. What is photoinhibition? Some insights from comparisons of shade and sun plants. In: Baker NR, Bowyer NR, eds. *Photoinhibition of photosynthesis*. Oxford: Bios, 1–24.
- Pérez-Lloréns JL, Vergara JJ, Pino RR, Hernández I, Peralta G, Niell FX.** 1996. The effect of photoacclimation on the photosynthetic physiology of *Ulva curvata* and *Ulva rotundata* (Ulvales, Chlorophyta). *European Journal of Phycology* **31**, 349–359.
- Pérez-Rodríguez E, Gómez I, Karsten U, Figueroa FL.** 1998. Effects of UV-radiation on photosynthesis and excretion of UV-absorbing compounds of *Dasycladus vermicularis* (Dasycladales, Chlorophyta) from southern Spain. *Phycologia* **37**, 379–387.
- Pfündel E, Pan RS, Dilley RA.** 1992. Inhibition of violaxanthin de-epoxidation by ultraviolet-B radiation in isolated chloroplasts and intact leaves. *Plant Physiology* **98**, 1372–1380.
- Quintern LE, Horneck G, Eschweiler U, Bücker H.** 1992. A biofilm used as ultraviolet-dosimeter. *Photochemistry and Photobiology* **63**, 74–78.
- Ruban AV, Horton P.** 1994. Regulation of non-photochemical quenching of chlorophyll fluorescence in plants. *Australian Journal of Plant Physiology* **22**, 221–230.
- Schmid R, Dring MJ.** 1996. Blue light and carbon acquisition in brown algae: an overview and recent developments. *Scientia Marina* **60**, 115–124.
- Schmitz G, Schmidt M, Feierabend J.** 1996. Comparison of the expression of a plastidic chaperonin 60 in different plant tissues and under photosynthetic and non photosynthetic conditions. *Planta* **200**, 326–334.
- Schreiber U, Bilger W, Neubauer C.** 1994. Chlorophyll fluorescence as a non-intrusive indicator for rapid assessment of *in vivo* photosynthesis. *Ecological Studies* **100**, 49–70.
- Sokal RR, Rohlf FJ.** 1995. *Biometry. The principles and practice of statistics in biological research*, 3rd edn. New York: Freeman.
- Thayer SS, Björkman O.** 1990. Leaf xanthophyll content and composition in sun and shade determined by HPLC. *Photosynthesis Research* **23**, 331–344.
- van de Poll WH, Eggert A, Buma AGJ, Breeman AM.** 2001. Effects of UV-B-induced DNA damage and photoinhibition on growth of temperate marine red macrophytes: habitat-related differences in UV-B tolerance. *Journal of Phycology* **37**, 30–37.

- Vass I.** 1997. Adverse effects of UV-B light on the structure and function of the photosynthetic apparatus. In: Pessaraki M, ed. *Handbook of photosynthesis*. New York: Marcel Dekker Inc, 931–949.
- Vergara JJ, Pérez-Lloréns JL, Peralta G, Hernández I.** 1997. Seasonal variation of photosynthetic performance and light attenuation in *Ulva* canopies from Palmones river estuary. *Journal of Phycology* **33**, 773–779.
- Vergara JJ, Sebastian M, Pérez-Lloréns JL, Hernández I.** 1998. Photoacclimation of *Ulva rigida* and *U. rotundata* (Chlorophyta) arranged in canopies. *Marine Ecology Progress Series* **165**, 283–292.
- Young AJ, Frank HA.** 1996. Energy transfer reactions involving carotenoids: quenching of chlorophyll fluorescence. *Journal of Photochemistry and Photobiology B: Biology* **36**, 3–15.